Analytical Methods

Accepted Manuscript

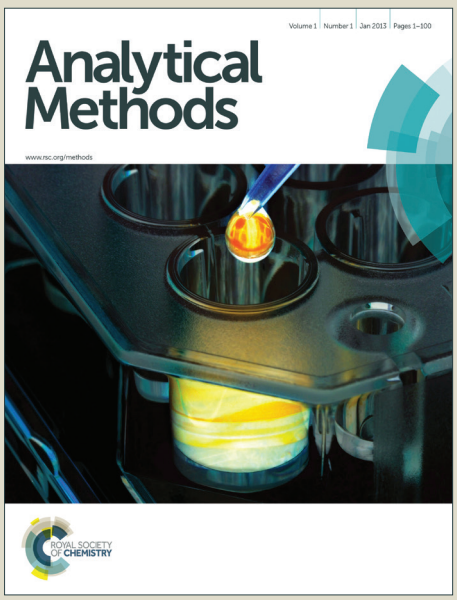

ROYAL SOCIETY OF CHEMISTRY

www.rsc.org/methods

Table of Contents Entry

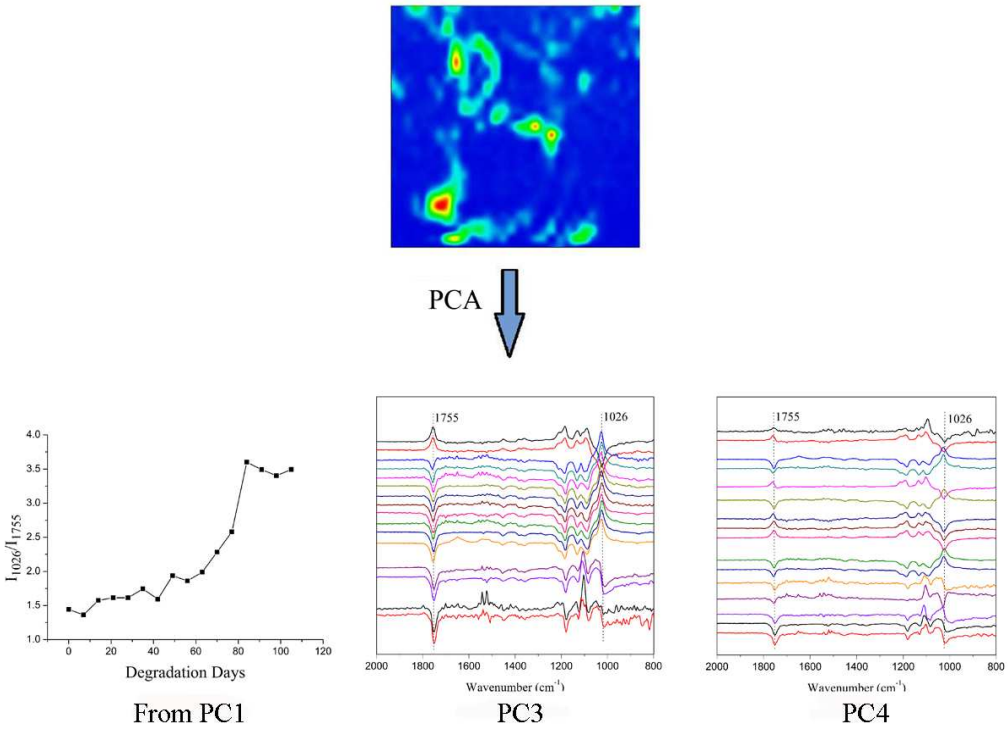

This paper proposes coupling ATR/FTIR mapping with principal component analysis for the biomimetic degradation of porous poly(L-lactide)/hydroxyapatite (PLLA/HA) composite material.

Attenuated Total Reflectance/Fourier Transform Infrared (ATR/FTIR) Mapping Coupled with Principal Component Analysis for the Study of *In Vitro* Degradation of Porous Polylactide/Hydroxyapatite Composite Material

Nan Jing, Xiaoting Jiang, Qian Wang, Yongjiao Tang and Pudun Zhang*

Abstract:

Attenuated total reflectance/Fourier transform infrared (ATR/FTIR) mapping was used to characterize the degradation of porous polylactide/hydroxyapatite (PLLA/HA) composite material. The ATR/FTIR images were acquired using a Continuμm XL FTIR imaging microscope coupled with a Slide-On Si ATR accessory at a resolution of 8 cm^{-1} with 8 co-added scans in the wavenumber range of 4000–650 cm^{-1}. Principal component analysis (PCA) method was used to analyze the FTIR image data. Four principal components (PCs) were identified by analyzing both the scree plot and the loading spectra. The degradation at varied days was clearly described by the curve of the intensity ratio of the band at 1026 cm^{-1} to the one at 1755 cm^{-1} (I_{1026}/I_{1755}) in the first PC's (PC1's) loading plot versus the days. The shape and position of the second PC (PC2) is similar to the IR spectrum of water, implying that it comes from the contribution of water absorbed on the porous sample. The variations of the bands at 1755 cm^{-1} and 1026 cm^{-1} in PC3's loading plots reflected the changes of PLLA and

* *State Key Laboratory of Chemical Resource Engineering, Analysis & Test Center, Beijing University of Chemical Technology, E-mail: zhangpd@mail.buct.edu.cn*

HA in different days, respectively, while the fourth PC (PC4) suggested a transition from the abstract signal to the noise. These results demonstrate that ATR/FTIR mapping coupled with PCA could effectively characterize the degradation process of porous PLLA/ HA composite material.

1 Introduction

Fourier transform infrared (FTIR) spectroscopic imaging is a chemical imaging technique developed in recent twenty years[1] for detecting the distribution of chemical components of a sample in a micro-region. It expands traditional FTIR technique from "point" analysis to "plane", even "stereoscopic" analysis. This technique can be achieved by mapping or imaging on the basis of the adopted detector.[2] As with traditional FTIR method, three collecting modes, *i.e.* transmission, reflection and attenuated total reflectance (ATR), are provided for FTIR mapping or imaging. FTIR imaging has been applied in life sciences,[3-6] biomedical science,[7-9] polymers,[10-13] artworks and archeology,[14-16] and forensic science,[17,18] etc.

Univariate analysis is often used in exploring FTIR images, in which one or two characteristic absorption bands of a particular component are selected to build visual chemical image and further to obtain the composition and distribution information of components in a sample.[19] Though this method is simple and easy-to-understand, it cannot accurately reflect the compositions and distribution of a multi-component sample or a sample with complex structure because of the spectral overlapping. More importantly, since only one or two absorption bands are used, much of the information

is sacrificed and thus it can not represent the whole spectral and spatial distribution of the components in some cases. Principal component analysis (PCA) is a commonly used multivariate analysis method.[20-22] When being used in processing FTIR images, it regards each spectrum (pixel) as a whole rather than just considering individual absorption band in a spectrum. PCA decomposes the spectral data matrix of an image into the product of loading and score of a series of principal components (PC), which represent the spectrum and the concentration distribution of each abstract pure component, respectively.

Hydroxyapatite (HA) is an important biocompatible inorganic component of bone and tooth of vertebrates.[23] Poly(L-lactide) (PLLA) is a nontoxic polymer and it can be degraded into CO_2 and H_2O under wet conditions, which are not harmful to human. Just because of their excellent biocompatility, PLLA/HA porous composite materials are often used as scaffolds for bone tissue engineering.[24] However, to guarantee a healthy growth of bone, the degradation rate of scaffold must be adapted to the growth of tissue during the bone-repair process. Due to the great limitations and the strict and severe conditions for *in vivo* study, most of the degradation was *in vitro* investigated under biomimetic condition.[25,26] The *in vivo* degradation of the composite material can be well predicted from the *in vitro* results. In this work, ATR/FTIR mapping coupled with PCA was used to study the *in vitro* degradation of PLLA/HA composite material and to further analyze the changes of chemical composition during the degradation process. Different from our previous work,[27] this presented manuscript systematically explored the application of PCA in analysis of the FTIR images. PCA

can highlight the subtle but important changes of the spectra that are often difficult to be observed using univariate methods. Therefore it is an expectable approach to characterize the degradation of PLLA/HA composites. Our result demonstrates that some interesting and meaningful results were obtained by using this method.

2 Experimental

2.1 Instruments, materials and reagents

A Thermo Nexus 8700 FTIR spectrometer coupled with a Continuμm XL FTIR imaging microscope (Thermo Electron, WI, USA) was used to collect the FTIR images. The microscope was allocated with a Slide-on Si ATR accessory (Thermo Electron, USA). The biomimetic degradation was conducted in a DK-420S three-way water bath (Shanghai Jinghong, China). Poly(L-lactide) with an inherent viscosity (η) of 1.22 dl/g and a weight-average molecular weight (M_w) of about 121,000 g/mol was purchased from Jinan Daigang Biomaterials Co. Ltd. (Jinan, China). The rod-like nano-HA powder with an average length of 150 nm and width of 20 nm was obtained from Nanjing Emperor Nano Materials Co. Ltd (Nanjing, China). 1,4-Dioxane, $AgNO_3$, NaCl, KCl, Na_2HPO_4 and KH_2PO_4 were of analytical grade.

2.2 Preparation of PLLA/HA composite material

Solvent casting/salt leaching method[27,28] was used to prepare the porous PLLA/HA composite material. PLLA and HA were first ultrasonically dispersed in two same volume of dioxane, the two solutions were then mixed together under vigorous magnetic stirring. The ground NaCl powder with particle size of 150-200 μm (80-100

mesh) was added as the porogen into the mixed suspension and continued to stir till the suspension became homogeneous. The as-prepared mixture was cast onto the petri dishes to a thickness of about 1 mm and then dried at room temperature. The dried samples were soaked into deionized water to remove the salt. The water was replaced by the fresh one every 12 hours till the residual chloride ion was no longer detected. Finally, the obtained composite materials were dried in a vacuum oven at 45 ^{o}C for 48 h.

2.3 *In vitro* degradation of PLLA/HA composite material

PLLA/HA composite materials were immersed in phosphate buffered saline (PBS) solution (pH=7.4) at 37 ^{o}C for *in vitro* degradation. A few pieces of sample were taken out every 7 days and were rinsed with deionized water to remove the residual PBS salts. The buffer solution was simultaneously replaced by the fresh one. The as-treated materials were dried in a vacuum oven at 45 ^{o}C for 24 h.

2.4 ATR/FTIR mapping

The dried PLLA/HA samples were cut into sheets with a size of 1 cm × 1 cm and was fixed onto a glass slide using a double-sided adhesive tape, which was placed on the stage of FTIR imaging system and was detected using a liquid nitrogen-cooled mercury cadmium telluride (MCT) detector. A Slide-on Si ATR accessory was mounted on a 15 × IR objective (N.A.=0.58) for collecting ATR/FTIR images. Before collection, the Si ATR element was pulled out in order that the beams were focused on the sample. The mapping area with a size of 300 μm × 300 μm was selected in the bright field of view and then the ATR element was pushed in. The ATR/FTIR images

were acquired with a pixel size of 10 μm at a resolution of 8 cm^{-1} with 8 co-added scans in the wavenumber range of 4000–650 cm^{-1}, implying that 961 spectra (31 × 31) was involved in an ATR/FTIR image. The scanning step was triggered once the Si element was contacted with the sample surface. The acquiring, the processing and the analysis of the ATR/FTIR images were implemented using the Atlμs software of Omnic 7.2 (Thermo Electron). It was stressed that the mapping areas are not the same at each time because all the FTIR images were off-line collected. The collection of ATR/FTIR images at different area/location is better than at only one micro-region to characterize the degradation behavior.

3 Results and discussion

3.1 ATR/FTIR spectra of PLLA and HA

Fig.1 shows the ATR/FTIR spectra of PLLA, HA and their mixture. The bands at 1755 cm^{-1}, 1184 cm^{-1} and 1088 cm^{-1} in PLLA's spectrum arising from the stretch vibration of the C=O group ($\nu_{C=O}$), the asymmetric and symmetric stretch vibrations of the C-O-C group ($\nu_{as(C-O-C)}$ and $\nu_{s(C-O-C)}$), respectively; while the band at 1026 cm^{-1} attributes to the stretch vibration of the P-O group of HA. It is observed that this band is overlapped with the one at 1044 cm^{-1} (ν_{C-CH3}) of PLLA in the spectrum of their mixture.

Fig. 1

3.2 Interpretation of ATR/FTIR image

Fig.2 (a) shows an ATR/FTIR image of non-degrading PLLA/HA composite. Since degradation always occurred on PLLA and HA remained unchanged throughout the degradation process, all the FTIR images involved in this paper are generated based on the absorption band of the carbonyl group of PLLA at 1755 cm^{-1}. Fig.2 (b) shows the color scale in which the absorbance sequentially increases from blue to red.

An FTIR image contains large amounts of spectral information in which each pixel corresponds to an infrared spectrum. Fig.2(c) shows the infrared spectra in different pixels in Fig.2(a). The blue area has no any absorption signal other than noise, representing the pore region of the composite; while other color areas show the spectra of the mixture of PLLA and HA, suggesting the pore walls of the composite.

Fig. 2

3.3 The principle of PCA for FTIR image

FTIR image data usually consist of four dimensions, *i.e.* *x*- and *y*- dimensions (defining the spatial position), a spectral dimension (describing the chemical information of components) and an intensity dimension (corresponding to the concentration of component). These raw data cannot be completely displayed on three-dimensional images, thus a big challenge in analysis of FTIR image is how to effectively extract information from these hyperspectral images.

The spectrum of a pixel in FTIR image is essentially the weighted sums of the

product of each pure spectrum by the concentration of the pure component in this pixel based on the Beer-Lambert law. Although the concentration of each pure component varied with pixel, the spectra are identical. FTIR image data can be expressed using a matrix $\mathbf{D=CS^T+E}$, where **D** is the original experimental data matrix with a size that equals the number of pixel × number of wavenumbers, C the concentration matrix of the components with a size that equals the number of pixel × number of components, $\mathbf{S^T}$ the spectral matrix consisting of the spectra of pure components with a size that equals number of components × number of wavenumbers, and **E** is the error matrix. All of the image data are mean-centered by spectrum before PCA and are then linearly decomposed into a few uncorrelated new variables (*i.e.* PCs). The new variables are ranked by decreasing order of contribution to total variance, meaning that the first PC (PC1) covers the largest variance and PC2 covers the second largest variance and so forth. After PCA, the FTIR image data are expressed as matrix $\mathbf{D=TP^T+E}$, where **T** is the score matrix, in which the column vectors can be folded back to form the score maps, representing the abstract concentration distribution; while $\mathbf{P^T}$ is the loading matrix, in which the row vectors represent the abstract pure spectra.[29] The loading plots are usually associated with infrared spectra,[30,31] in which the positive or negative bands indicate that certain characteristics are appearing or missing in the corresponding PCs.

3.4 Determination of the number of PCs

In principle, the number of PCs is no larger than the number of wavenumbers. However, since experimental errors always exist when acquiring FTIR image, only

the first few PCs can describe the spectral variations relating to the chemical composition, others are the contribution of noise. Therefore, how to determine the number of PCs is an important issue for analyzing FTIR image. Scree plot is one of the often used methods,[20] in which a plot of the eigenvalue (or the fraction of total variance) of each PC versus the serial number of PC is created. Generally only the first few PCs has large eigenvalues and thus show a steep slope in the scree plot, other PCs forms a "scree-like" platform due to their small eigenvalues. The PCs before inflexion in the scree plot are usually selected for PCA. Fig. 3 shows the scree plot of PLLA/HA composite at day 84, which indicates that only PC1 is the valuable component. Similar results were also achieved by analyzing the composites in other degradation days. This method had been successfully applied in our previous work.[13]

Fig. 3

Nevertheless, when observing the loading plots (Fig. 4), we find that they do not display the noise until PC5; while for PC2-PC4, some "characteristic bands" are still shown in the loadings even though their eigenvalues are small. These results imply that determination of the number of PCs using scree plot method may sometimes leads to the loss of some valuable PCs. A solution to this problem is to compare the loadings with the infrared spectra of the real components and retain the PCs that show the "characteristic bands" in loadings.[20] On the basis of this principle, PC1 to PC4 may be retained, however, the shape and position of the loading plot of PC2 is similar

to the IR spectrum of water, implying that it might be derived from the adsorption of water on the porous material during the collection.

Fig.4

3.5 Principal component analysis for the degradation of PLLA/HA composite material

For samples at every degradation day, the PCA results show that PC1 covers more than 90% of the total variance and the loading plot (Fig.5(a)) contains nearly the entire characteristics of the spectrum of the mixture of PLLA and HA, which represents the average spectrum of the image. Correspondingly, the score map of PC1 (figure not shown) also reflects the distribution of the predominant component, which is almost consistent with the ATR/FTIR image based on a characteristic band (image not shown). Further, a degradation curve of the intensity ratio of the band at 1026 cm^{-1} to the one at 1755 cm^{-1} in the loadings of PC1 (I_{1026}/I_{1755}) versus the degradation days is achieved (Fig.5(b)). It indicates that this ratio increases slowly before day 56, suggesting a slow degradation is occurred in this stage. During the period 56-84 day, this ratio increases rapidly, suggesting the degradation is accelerated. The acceleration of the degradation might result from the hydrolysis of the polymer which can auto-catalyze the degradation.[32] These ratios become stable after day 84, suggesting that some of the HA might be peeled off from the pore walls.

Fig.5

The loading plots of PC3 of the FTIR images at different degradation days are shown in Fig. 6. The band at 1755 cm^{-1} corresponds to the characteristic absorption of C=O group in PLLA and is positive at day 0 and 7, indicating that the degradation has not yet been initiated. From the 14th day, the band becomes negative and gradually increases with the days, suggesting that the content of PLLA is reduced with the increase of degradation days. Compared with our previous work that the change of morphology cannot be observed until day 28,[28] ATR/FTIR mapping coupled with PCA can reflect the degradation of composite more effectively. Since the significant degradation of PLLA in the late period resulted in a fragmentation of the sample, it is difficult to collect an ATR/FTIR image after day 105. In addition, the band at 1026 cm^{-1} in the loadings of PC3 is caused by HA and is nearly unchanged during the period 14-77 day. However, it changes to negative band after day 84, suggesting a decrease of HA's content. This result is identical to the one drawn from the degradation curve (Fig. 5(b)).

Fig. 6

Fig.7 shows the loading plots of PC4 at different degradation days. All the bands at 1755 cm^{-1} show negative values till the materials are degraded more than 63 days, which is consistent with our previous study on the degradation half-life.[28] Since the

eigenvalues of all the PC4 are low (<1.6%), it is essentially a minor factor that transits from the abstract signal to the noise. the variations of the bands (positive or negative) before day 63 may be caused by the big noise during the collection of FTIR images. These small eigenvalues can also be applied to interpret the variations of the band at 1026 cm^{-1} in PC4.

Fig. 7

4. Conclusion

ATR/FTIR mapping coupled with PCA was used to study the degradation of porous PLLA/HA composite material. Four PCs were identified by analyzing both the scree plot and the loadings of the images. The loading plot of PC1 represents the average spectrum of an image. The degradation curve based on the ratio of the band at 1026 cm^{-1} to the one at 1755 cm^{-1} (I_{1025}/I_{1755}) in the loading plots of PC1 versus the days indicates that the degradation is slow in the first 56 days and is accelerated during the period 56-84 day. However, the degradation becomes stable after day 84. PC2 attributes to the water absorbed on the sample. Both PC3 and PC4 show the variations of the characteristic bands of PLLA and HA during the degradation process. The loadings of PC3 suggest that the degradation of the composite starts from day 14. In addition, PC4 reflects a transition from the abstract signal to the noise and the variations of the bands (positive or negative) in PC4 are caused by the experimental noise. All other PCs (e.g. PC5 to PC8) only reflect the experimental noise. Our results

indicate that ATR/FTIR mapping coupled with PCA is an effective method for characterizing the degradation of PLLA/HA composite material. Combining further with some quantitative approaches, it is possible to quantitatively describe the degradation process and establish a degradation model.

References

1 E. N. Lewis, P. J. Treado, R. C. Reedor, G. M. Story, A. E. Dowrey, C. Marcott and I. W. Levin, *Anal. Chem.*, 1995, **67**, 3377-3381.

2 R. Bhargava, B. G. Wall and J. L. Koenig, *Appl. Spectrosc.*, 2000, **54**, 470-479.

3 P. Yu, *J. Struct. Biol.*, 2005, **150**, 81-89.

4 M. Z. Kastyak-Ibrahim, M. J. Nasse, M. Rak, C. Hirschmugl, M. R. Del Bigio, B. C. Albensi and K. M. Gough, *NeuroImage*, 2012, **60**, 376-383.

5 G. Cakmak, L. M. Miller, F. Zorlu and F. Severcan, Amifostine, *Arch. Biochem. Biophys.*, 2012, **520**, 67-73.

6 M. J. Hackett, J. Lee, F. El-Assaad, J. A. McQuillan, E. A. Carter, G. E. Grau, N. H. Hunt and P. A. Lay, *ACS Chem. Neurosci.*, 2012, **3**, 1017-1024.

7 R. Noreen, M. Moenner, Y. Hwu and C. Petibois, *Biotechnol. Adv.*, 2012, **30**, 1432-1446.

8 Y. Kobrina, L. Rieppo, S. Saarakkala, J. S. Jurvelin and H. Isasson, *Osteoarthr. Cartilage*, 2012, **20**, 460-468.

9 N. Bergner, B. F. M. Romeike, R. Reichart, R. Kalff, C. Krafft and J. Popp,

Analyst, 2013, **138**, 3983-3990.

10 A. Gupper and S. G. Kazarian, *Macromolecules*, 2005, **38**, 2327-2332.

11 X. Zhou, P. D. Zhang, Z. F. Li and G. Y. Rao, *Anal. Sci.*, 2007, **23**, 877-880.

12 X. Zhou, P. D. Zhang, X. T. Jiang and G. Y. Rao, *Vib. Spectrosc.*, 2009, **49**, 17-21.

13 Y. M. Zhou, B. B. Li and P. D. Zhang, *Appl. Spectrosc.*, 2012, **66**, 566-573.

14 K. Keune and J. J. Boon, *Anal. Chem.*, 2004, **76**, 1374-1385.

15 A. van Loon and J. J. Boon, *Spectrochim. Acta B*, 2004, **59**, 1601-1609.

16 R. Mazzeo, E. Joseph, S. Prati and A. Millemaggi, *Anal. Chim. Acta.*, 2007, **599**, 107-117.

17 K. L. A. Chan and S. G. Kazarian, *Analyst*, 2006, **131**, 126-131.

18 C. Ricci, S. Bleay and S. G. Kazarian, *Anal. Chem.*, 2007, **79**, 5771-5776.

19 C. Gendrin, Y. Roggo and C. Collet, *J. Pharmaceut. Biomed.*, 2008, **48**, 533-553.

20 D. Clark and S. Šašic, *Cytom. Part A*, 2006, **69A**, 815-824.

21 H. Shinzawa, K. Awa, W. Kanematsu and Y. Ozaki, *J. Raman Spectrosc.*, 2009, **40**, 1720-1725.

22 J. M. Prats-Montalbán, A. de Juan and A. Ferrer, *Chemometr. Intell. Lab. Syst.*, 2011, **107**, 1-23.

23 I. S. Neira, Y. V. Kolen'ko, O. I. Lebedev, G. V. Tendeloo, H. S. Gupta, F. Guitian and M. Yoshimura, *Cryst. Growth Des.*, 2009, **9**, 466-474.

24 Z. K. Hong, P. B. Zhang, C. L. He, X. Y. Qiu, A. X. Liu, L. Chen, X. S. Chen and X. B. Jing, *Biomaterials*, 2005, **26**, 6296-6304.

25 T. Niemelä, H. Niiranen and M. Kellomäki, *Acta Biomaterialia*, 2008, **4**, 156-164

26 Y. S. Liu, Q. L. Huang, A. Kienzle, W. E. G. Müller, Q. L. Feng, *Mater. Sci. Eng. C,* 2014, **38**, 227-234.

27 Q. Wang, X. T. Jiang, Y. Z. Xin, J. X. Cui and P. D. Zhang, *Chinese J. Anal. Chem.*, 2014, **42**, 221-226.

28 X. T. Jiang, Q. Wang and P. D. Zhang, *Chemical Research and Application*, 2011, **6(23)**, 755-760. (in Chinese)

29 M. R. Keenan, in: H. F. Grahn, P. Geladi (Eds), Techniques and applications of hyperspectral image analysis, John Wiley & Sons Ltd, Chichester, 2007, pp. 97-102.

30 J. Sorber, G. Steiner, V. Schulz, M. Guenther, G. Gerlach, R. Salzer and K. Arndt, *Anal. Chem.*, 2008, **80**, 2957-2962.

31 M. S. Lindblad, B. M. Keyes, L. M. Gedvilas, T. G. Rials and S. S. Kelley, *Cellulose*, 2008, **15**, 23-33.

32 X. L. Xu, X. S. Chen, A. X. Liu, Z. K. Hong and X. B. Jing, *Euro. Polym. J.,* 2007, **43**, 3187-3196.

1

Figure Captions

Fig.1 FTIR spectra of PLLA, HA and their mixture.

Fig.2 FTIR image of non-degrading PLLA/HA composite material

a) FTIR image based on the absorption band at 1755cm^{-1}; b) the color scale; and c) FTIR spectra of different pixels in the image.

Fig.3 The scree plot of the FTIR image of the PLLA/HA composite at day 84.

Fig.4 Loading plots of the first eight PCs of the FTIR image of PLLA/HA composite materials at day 84.

Fig.5 (a) The loading plots of PC1 of the ATR/FTIR images at day 0, 7, 14, 21, 28, 35, 42, 49, 56, 63, 70, 77, 84, 91, 98 and 105 (from top to bottom). (b) Degradation curve of I_{1026}/I_{1755} versus the degradation days.

Fig.6 The loading plots of PC3 of the FTIR images at day 0, 7, 14, 21, 28, 35, 42, 49, 56, 63, 70, 77, 84, 91, 98 and 105 (from top to bottom).

Fig.7 The loading plots of PC4 of the FTIR images at day 0, 7, 14, 21, 28, 35, 42, 49, 56, 63, 70, 77, 84, 91, 98 and 105 (from top to bottom)

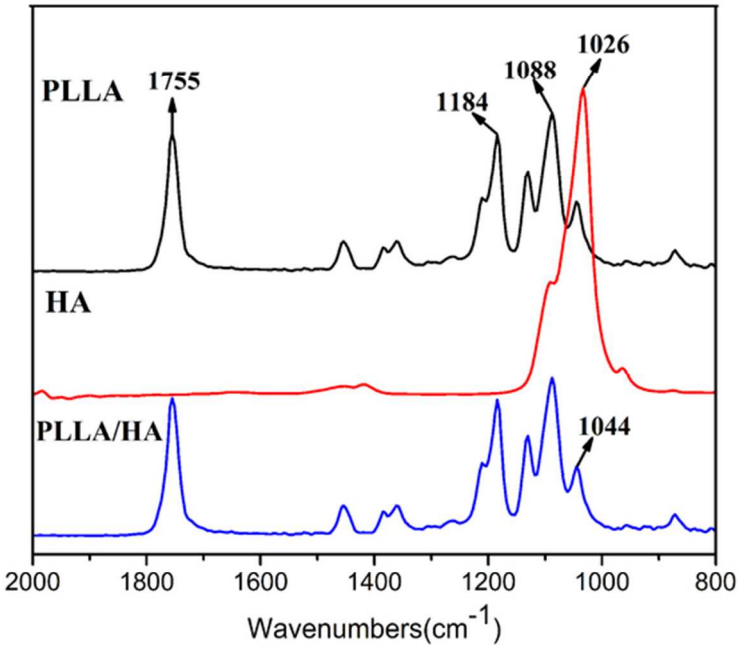

Fig.1
63x44mm (300 x 300 DPI)

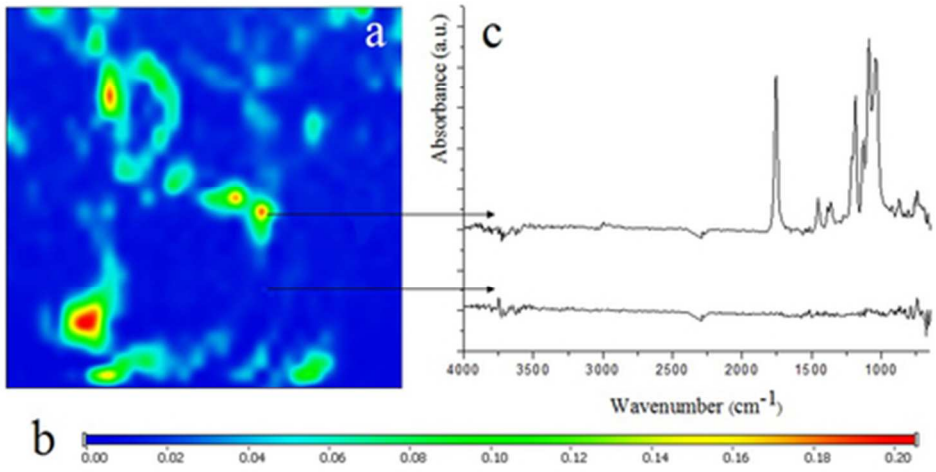

Fig.2
42x21mm (300 x 300 DPI)

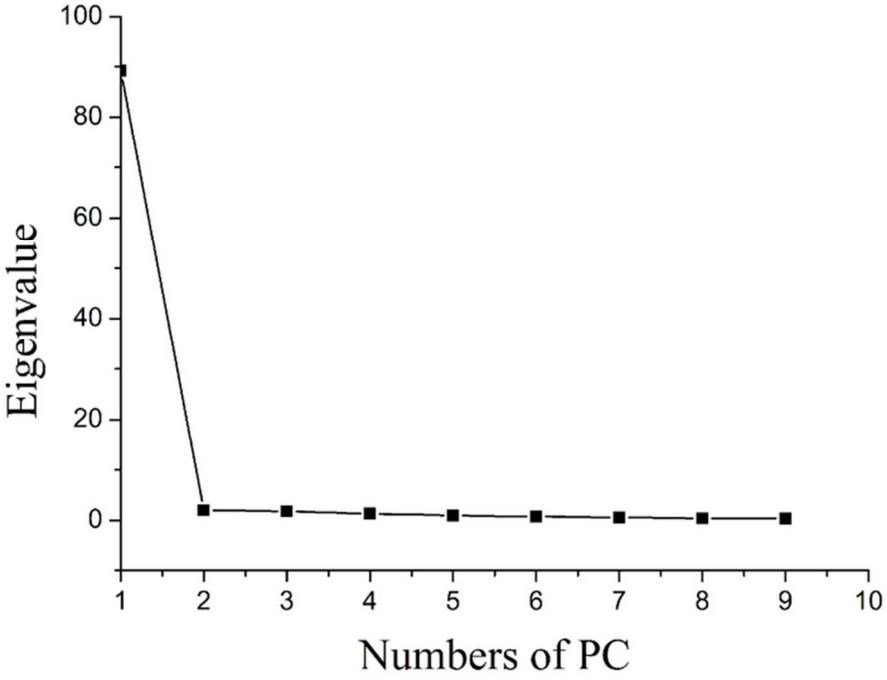

Fig.3
67x53mm (300 x 300 DPI)

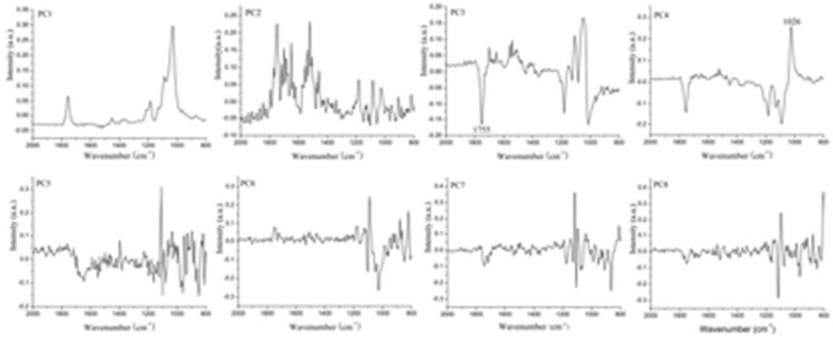

Fig.4
35x15mm (300 x 300 DPI)

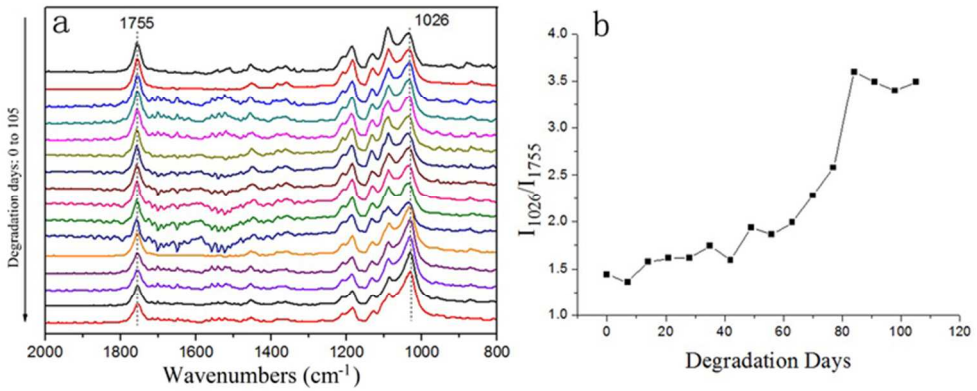

Fig.5
68x27mm (300 x 300 DPI)

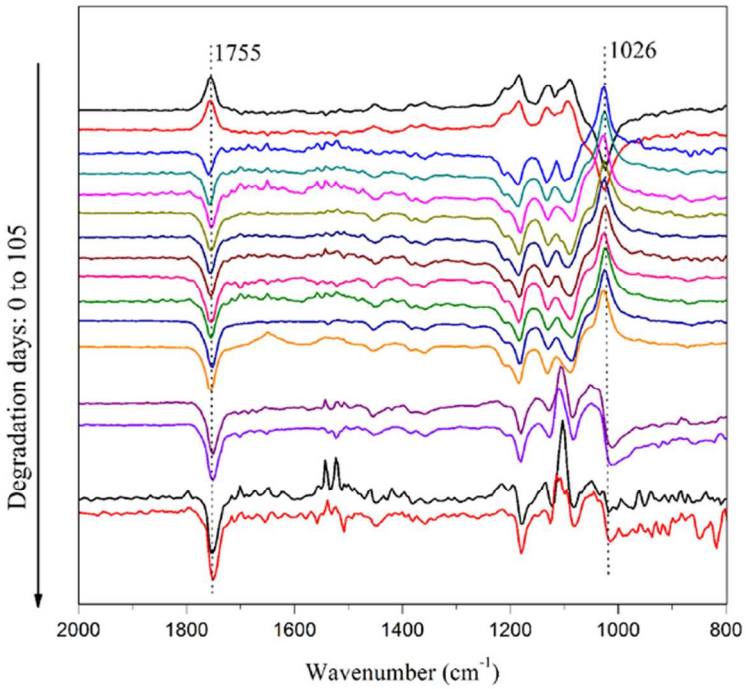

Fig.6
68x48mm (300 x 300 DPI)

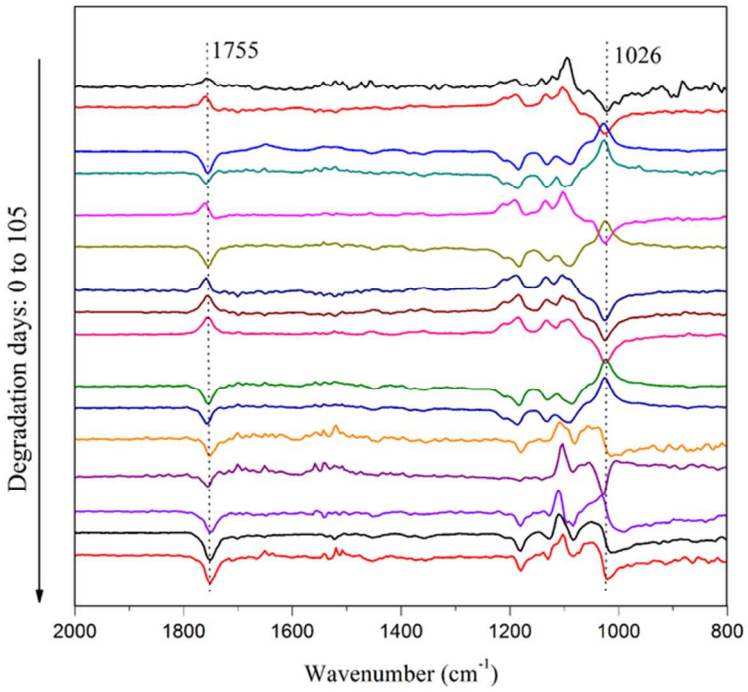

Fig.7
68x48mm (300 x 300 DPI)